Illumination as a tool to investigate the quantum mobility of the two-dimensional electron gas in a Si δ-doped GaAs/$In_{0.15}Ga_{0.85}As$/GaAs quantum well

A. Cavalheiro,[1] E. C. F. da Silva,[2] E. K. Takahashi,[1] A. A. Quivy,[2] J. R. Leite,[2] and E. A. Meneses[3]
[1]*Departamento de Ciências Físicas da Universidade Federal de Uberlândia, CP 595, 38400-902 Uberlândia, MG, Brazil*
[2]*Instituto de Física da Universidade de São Paulo, CP 66318, 05315-970 São Paulo, SP, Brazil*
[3]*Instituto de Física Gleb Wataghin, Universidade Estadual de Campinas, CP 6165, 17083-970 Campinas, SP, Brazil*
(Received 9 April 2001; revised manuscript received 4 September 2001; published 1 February 2002)

A systematic investigation of the transport properties of a GaAs/InGaAs quantum well electronically coupled to a silicon delta-doped layer was carried out as a function of the illumination time of the sample. Shubnikov–de Haas measurements allowed the determination of the quantum mobility of each occupied subband that could be accurately analyzed from the dark condition up to the continuous-illumination regime. The origin of the persistent-photoconductivity effect observed in the sample could be unambiguously determined and was confirmed by self-consistent calculations.

DOI: 10.1103/PhysRevB.65.075320 PACS number(s): 78.55.−m

I. INTRODUCTION

Delta-doped (δ-doped) heterostructures have been extensively investigated due to their potential applications to high-performance devices and to their interesting physical properties.[1] Particularly, a phenomenon which has attracted the attention of many researchers is the persistent-photoconductivity (PPC) effect observed in δ-doped based semiconductor materials.[2–10] Although such an effect has already been extensively investigated, up to date no satisfactory model was able to point out the physical mechanisms that might be involved. The origin of the PPC effect in semiconductor layers with a single Si δ-doped plane is still under debate, as can be seen in the papers available on the subject.[2–6] The problem is more interesting and controversial when a δ-doped layer is placed close to a quantum well (QW). In this case, the characterization of the system is much more complicated due to the presence of two possible conducting channels and to the transfer of electrons from one channel to the other one. For the specific case of a Si δ-doped GaAs/InGaAs/GaAs quantum well, the physical mechanisms responsible for the PPC effect are still unclear.[9,10] Babinski *et al.*[9] found that a fraction of the two-dimensional electron gas (2DEG) was trapped on deep centers within the structure at room temperature and could not be detected at low temperature. Recently, Zervos *et al.*[10] explained the PPC effect observed in their samples in terms of electrostatic band bending caused by the capture of photoexcited holes by background acceptorlike impurity states and/or the photoionization of deep states. As a consequence, it can be inferred from all the works cited above that the PPC effect in δ-doped GaAs-based heterostructures is still not well understood and certainly requires further investigations to clearly identify its origin. In the present work, we show that, in a system where a δ layer is located close to a $In_{0.15}Ga_{0.85}As$ QW, the electrical conduction can give rise to interesting effects which are due to the interplay between the two-dimensional carriers confined in the δ QW and the InGaAs QW. Using the illumination as a tool, we were able to follow, in an accurate way, the evolution of the quantum mobility of each electronic subband of the system. Our experimental data clearly demonstrate that usual transport measurements carried out only under two different illumination conditions (generally in the dark and under continuous illumination) might be misleading, and a detailed study as a function of the illumination time can be of great value.

II. EXPERIMENTAL DETAILS

A. Molecular-beam epitaxy growth

The sample structure designed for this study was grown on top of a GaAs(001) substrate and consists of a 1-μm-thick GaAs buffer layer grown at 570 °C followed by a $10\times(AlAs)_5(GaAs)_{10}$ superlattice grown at 600 °C, a 1000-Å-thick GaAs back barrier grown at 570 °C, a 150-Å-wide $In_{0.15}Ga_{0.85}As$ QW grown at 520 °C, a 20-Å-thick GaAs spacer, a silicon δ-doped layer with a nominal Si concentration $N_{Si}=4.0\times10^{12}$ cm^{-2}, and a GaAs top barrier of 500 Å, all of them grown at the same temperature as the InGaAs layer. In order to neutralize the surface states, the sample structure was capped with a 100-Å-thick n^+ GaAs layer ($n_{cap}=10^{17}$ cm^{-3}). The growth temperature was ramped down to 520 °C after the first GaAs barrier to avoid In evaporation from the surface and limit the diffusion of the dopant into the host material that could yield a broadening of the doping profile. The planar doping was achieved by the standard growth-interruption technique and simultaneous evaporation of the dopant. The growth was interrupted during 30 sec before the deposition of the Si layer in order to smooth the surface. The sample was grown with a V/III flux ratio of 5.

B. Shubnikov–de Haas measurements and data analysis

The magnetoresistance measurements were performed at 1.5 K in a bath cryostat inserted into a superconducting coil using a standard van der Pauw configuration. The magnetoresistance (R_{xx}) was measured using a 10-μA dc current and the sample was illuminated by a light-emitting diode (LED) whose photon energy ($\sim$1.74 eV) was larger than the band-gap energy of the GaAs material at 1.5 K

(~1.52 eV). The Shubnikov–de Haas (SdH) measurements were carried out under the following conditions: the first measurement was performed just after cooling down the sample in the dark. Next, the sample was illuminated for a short period of time and a second SdH measurement was performed in the dark. The same procedure (but with a longer and longer period of illumination followed by the SdH measurement in the dark) was applied several times until no significant change of the data could be observed.

These SdH measurements were used to obtain the density and the quantum mobility of the electrons in each subband. The experimental data were numerically differentiated, expressed as a function of the reciprocal magnetic field (1/B) and analyzed using a fast Fourier transform (FFT) algorithm. The electron subband densities n_i ($i=0,1,2,3,\ldots$) were related to the frequencies ν_i of the SdH oscillations by the expression $n_i=2e\nu_i/h$ where e is the electronic charge and h is Planck's constant. The total free-electron density n_s was determined by summing the individual electron density n_i of all the observed subbands, $n_s=\Sigma_i n_i$.

As will be seen in the sequence of this work, the use of a simple FFT procedure to determine the electronic density of the occupied subbands generally produces peaks that are very close to each other and thus difficult to distinguish and identify. In order to determine the concentration of each subband with more accuracy, our magnetoresistance traces were multiplied by a smooth window function before computing their FFT. The Hanning-window function $f_w(B^{-1}=x)=1/2\{1-\cos[2\pi(x-x_i)/(x_j-x_i)]\}$ was used and, as already reported by Henriques,[11] produced a better-resolved Fourier spectra. After separating the FFT peaks by previous filtering of the SdH data using the Hanning window, the quantum mobility of a specific subband was determined by the logarithmic dependence of the maximum amplitude of the FFT peak plotted against $1/B$. In these conditions, the slope of the straight line through the data is equal to π/μ_i. This procedure is more straightforward than the usual Dingle plot and produces more reliable data.

III. RESULTS AND DISCUSSION

Figure 1 shows the results of the SdH measurements for the different illumination time periods (T_{illum}). We can see that R_{xx} decreases gradually as a function of the illumination time (curves $a-f$) and reaches a saturated stage in the range $280\leqslant T_{illum}\leqslant 1240$ s (curves $g-i$). After the measurement performed at $T_{illum}=1240$ s, the sample was kept in the dark, inside the cryostat, during 27 h. After that time, a SdH measurement was performed in the dark and the recorded magnetoresistance showed the same trace as the one obtained for $T_{illum}=1240$ s. A further decrease of the magnetoresistance was observed when the experiment was performed in the presence of continuous illumination (curve j). To conclude the whole sequence of SdH measurements, we performed a last measurement *in the dark*, just after the one performed in the presence of continuous illumination and the trace was once more identical to the one measured at $T_{illum}=1240$ s. These results strongly indicate that there are two distinct photoconductivity effects in our sample: (i) a persistent effect in the range $0\leqslant T_{illum}\leqslant 1240$ s; (ii) a nonpersistent effect that is only present under continuous illumination and can be associated with a band-to-band excitation effect, i.e., with electron-hole pair photogeneration.

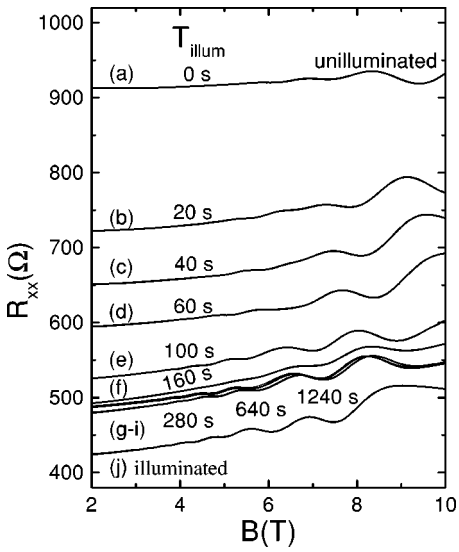

FIG. 1. Magnetoresistance (R_{xx}) of the sample measured at $T=1.5$ K: (a) just after cooling down the sample in the dark; (b)–(i) in the dark but after subsequent illumination periods, as indicated; (j) under continuous illumination. The SdH traces for $T_{illum}=280$, 640, and 1240 s are almost superimposed in this figure.

The SdH oscillations shown in Fig. 1 indicate the presence of a 2DEG in the active region of the sample, even before the sample exposure to any illumination (curve a). The data obtained after the simple FFT processing of the SdH curves are shown in Fig. 2(a) whereas the FFT spectra of the windowed data are presented in Fig. 2(b). Normally, the objective of the FFT of the windowed data is to provide a FFT spectrum with better resolved peaks in order to determine the occupation of each subband with a higher accuracy than in the case of the normal FFT procedure [compare Figs. 2(a) and 2(b)]. However, for computational reasons, the trace in the dark ($T_{illum}=0$ s) could not be processed in good conditions using the windowed FFT and only the main peak was resolved, although the first curve of Fig. 2(a) strongly suggests the presence of a shoulder around $n=1.0\times10^{12}$ cm^{-2} (that is related to the occupancy of the second subband, as will be demonstrated later). This computational artifact occurs because the FFT of the windowed curves generally provides better-resolved data at the expense of the intensity of the peaks related to the less occupied subbands.[11]

Let us initially assume that, at $T_{illum}=0$ s, there is only one occupied subband with an electron density $n_0=1.81\times10^{12}$ cm^{-2} as shown by the main peak of curve a in Fig. 2(a). After 20 s of illumination, another subband is clearly observed with an electron density $n_1=1.08\times10^{12}$ cm^{-2} [it now appears in Fig. 2(b) where the peaks are better resolved than in Fig. 2(a)]. Further illumination increases the population of the occupied subbands and, at $T_{illum}=280$ s, a third subband with $n_2=0.43\times10^{12}$ cm^{-2} is also observed. Due to the same computational problem already mentioned above, the FFT of the windowed data did not reveal the third sub-

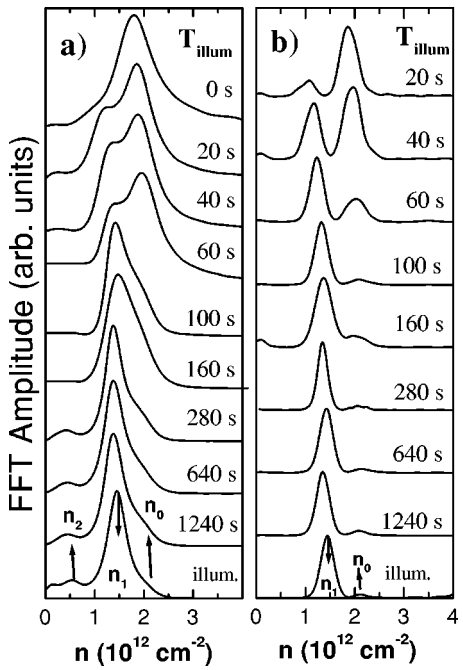

FIG. 2. FFT spectra of the traces shown in Fig. 1: (a) obtained using the simple FFT procedure; (b) obtained after windowing the magnetoresistance traces with the Hanning function. Although, in (a) three occupied subbands are detected during illumination, the windowed data only resolved two of them due to computational reasons (see text). The spectra have been vertically displaced for clarity.

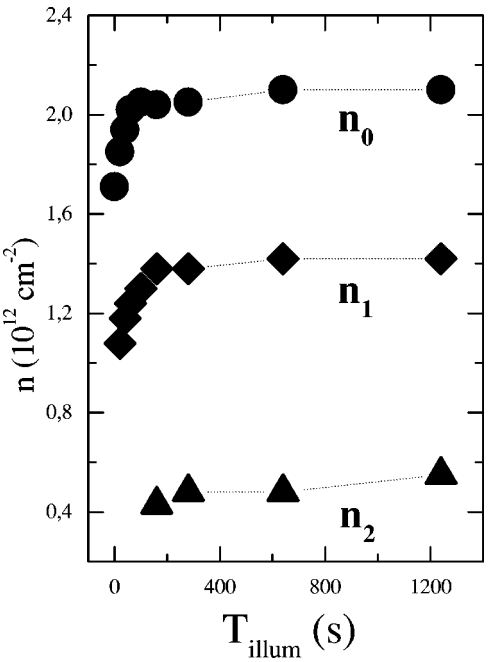

FIG. 3. Electron density of the first, second, and third subband as a function of the illumination time.

band, but its occupancy is clearly visible in Fig. 2(a) where the simple FFT was used. For $T_{illum}>280$ s, the illumination of the sample does not significantly alter the population of the three occupied subbands (the SdH traces for $T_{illum}=280$, 640, and 1240 s are practically superimposed in Fig. 1). When the measurement was performed in the presence of continuous illumination (curve *j* of Fig. 1), we observed an increase of approximately 0.1×10^{12} cm^{-2} in the total 2DEG concentration, mainly resulting from the increasing population of the third subband. After the light was turned off, this increment vanished and the active region recovered the same 2DEG concentration measured at $T_{illum}=1240$ s.

At $T_{illum}=0$ s, the total 2DEG density (if we consider only the main FFT peak related to the occupation of the lowest subband as initially assumed) is much smaller than the value obtained in our Hall measurement ($n_H=2.50\times10^{12}$ cm^{-2}) carried out under similar experimental conditions. Since the low-temperature Hall density always represents a lower limit to the total free-carrier density ($n_H\leq\Sigma_i n_i$), our larger value of n_H for $T_{illum}=0$ s is an indication that, even before any illumination of the sample, at least two subbands were already occupied in order to accommodate all the electrons detected by the Hall experiment. Although the peak related to the second subband was not resolved in the FFT of the windowed data, it is now clear from the Hall measurement that the shoulder observed in Fig. 2(a) at $T_{illum}=0$ s does correspond to the occupancy of the second subband with an electron concentration of about 1.0×10^{12} cm^{-2}. Therefore the total electron concentration of the 2DEG before exposure of the sample to any illumination is $n_s=2.81\times10^{12}$ cm^{-2}. In the presence of continuous illumination, $n_s=n_0+n_1+n_2=4.12\times10^{12}$ cm^{-2} is in excellent agreement with the nominal silicon concentration $N_{Si}=4.0\times10^{12}$ cm^{-2}.

The electron density of each subband extracted from the FFT spectra of the windowed (n_0 and n_1) and unwindowed (n_2) magnetoresistance data is presented in Fig. 3 as a function of the illumination time. In the present case, n_2 could be easily estimated from Fig. 2(a) because its value was much smaller than n_0 and n_1, and thus the peak associated to the third subband was well resolved. This figure clearly evidences the PPC effect which manifests itself as an increase of the electron density of the occupied subbands and as a saturation for large illumination periods. The total increment of carriers in the active region, in the interval $0\leq T_{illum}\leq1240$ s, is 1.19×10^{12} cm^{-2} considering that the population of the second subband at $T_{illum}=0$ s was equal to 1.0×10^{12} cm^{-2} as shown above. It is important to stress here that the significant changes in the subbands occupancy are not related to the presence of a parallel conducting channel since the width of the spacer layer separating the InGaAs QW and the δ-doped layer is only 20 Å. In this case, the InGaAs QW and the δ QW are coupled and the electronic wave functions are spread over both QW's simultaneously. In the case of parallel conduction, the δ plane and InGaAs QW are not coupled (because they are far from each other) and thus part of the electrons of the 2DEG cannot be detected by the SdH measurements due to their very low mobility in the δ QW.

The electron mobility of each subband of a 2DEG has already been determined by several groups in various δ-doped systems, and it always came out that its value was smaller in the lowest subband (the fundamental electronic

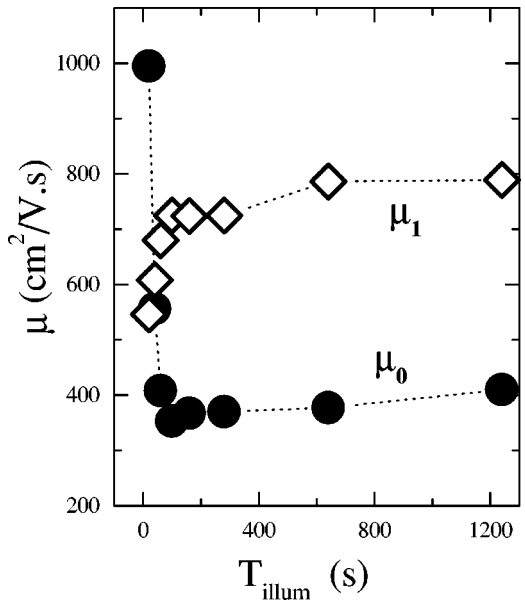

FIG. 4. Quantum mobility of the first and second subband as a function of the illumination time.

state) and increased with raising subband index.[6,12,13] These observations can be understood in terms of the physical extent of the electron distribution and in terms of their separation from the ionized donors: the electrons of the lowest subband are closer, in average, to the ionized impurities in the δ-doped layer and are thus scattered more strongly than those of the highest subbands that are less confined. Since the amplitude of the oscillatory magnetoresistivity consists of the prefactor $\exp(-\pi/\omega\tau)$, where $\omega = eB/m^*$ (m^* is the electronic effective mass), a higher FFT amplitude is related to a longer quantum lifetime τ and, consequently, to a larger value of the quantum mobility.[6,14] Therefore higher amplitudes of the FFT peaks should be expected for the highest subbands of the δ-doped systems. If we associate the shoulder present in the trace corresponding to $T_{illum}=0$ s in Fig. 2(a) to the occupancy of the second subband, our data are clearly contrary to the predicted trend because the quantum mobility of the carriers in the first subband is larger than the one in the second subband. Moreover, it can be seen in Fig. 2 that the relative amplitude of the Fourier peak associated with the lowest subband, which is initially larger than the one of the second subband, decreases with raising illumination time, indicating that the quantum electron mobility in that subband decreases with the increase of the 2DEG concentration.

In order to quantify the changes observed in the relative amplitude of the Fourier peaks presented in Fig. 2(b), the quantum mobility of each subband was determined using the procedure presented in Sec. II B and the results are shown in Fig. 4. The qualitative behavior observed in Fig. 2, i.e., the decreasing mobility of the lowest subband and the increasing mobility of the second one with the illumination time, is supported by the data presented in Fig. 4. Our results at $T_{illum}=20$ s are $\mu_0=995$ cm^2/V s and $\mu_1=546$ cm^2/V s, indicating that, at the beginning of the illumination process, the mobility of the lowest subband is larger than the one of the second subband. Moreover, if the data shown in Fig. 4 are extrapolated back to $T_{illum}=0$ s, we can state that, in the dark, the mobility of the fundamental subband has an even larger value than the one of the second subband. For large illumination periods, the system shows the usual behavior, i.e., the mobility increases with raising subband index. For instance, at $T_{illum}=1240$ s, $\mu_0=410$ cm^2/V s and $\mu_1=789$ cm^2/V s. In the presence of continuous illumination, an increase of both values is observed: $\mu_0=625$ cm^2/V s and $\mu_1=865$ cm^2/V s (not shown in the figure). As already explained above, computational artifacts did not allow the detection of the third sub-band in Fig. 2(b) and we were thus unable to compute its quantum mobility.

The large amount of carriers that is released by illumination (approximately 30% of the total 2DEG concentration) excludes the photoneutralization of negatively ionized acceptors in the GaAs layer surrounding the active region as the mechanism responsible for the PPC effect in our sample. Indeed, unintentionally doped GaAs layers grown by molecular beam epitaxy (MBE) are always lightly *p* type due to carbon (C) incorporation, and a background of 1×10^{15} cm^{-3} represents an upper limit of impurity concentration for samples grown by this technique. Such a small value is unable to explain the huge increase of carriers released by illumination. The major contribution of the acceptor photoneutralization to the increase of the total 2DEG concentration occurs when the measurement is performed under continuous illumination (curve *j* of Fig. 1). Before exposure of the sample to the radiation, the carbon acceptors are negatively charged in the GaAs region surrounding the δ and InGaAs QW's. Under continuous illumination, electron-hole pairs are created in the sample and the electrons flow towards the active region while the holes neutralize the negatively charged acceptors of the depleted GaAs layer. Once the light is turned off, the electrons are quickly recaptured by the acceptors and a decrease of 0.1×10^{12} cm^{-2} in the concentration of the 2DEG is observed. When the SdH measurement is performed under continuous illumination, there is a simultaneous increase of the mobility of the first and second subbands that mainly results from a reduction of the remote ionized-impurity scattering rather than from a strong band-edge modification induced by C neutralization. We can thus associate the carbon neutralization process to the nonpersistent photoconductivity effect observed in our sample.

Such a large number of carriers released by illumination (which is of the same order of magnitude as the concentration of Si atoms and deep traps in our sample) suggests three possible candidates to account for the PPC effect: (i) DX centers which are located within the narrow region of GaAs material where the Si donors of the δ layer are spread;[15] (ii) clustering of Si atoms in the δ-doped layer;[3,16] (iii) intrinsic deep donor traps spread out through the whole GaAs material with an energy level below the Fermi energy.[10,14]

It is known that, in GaAs, the DX-center energy level is resonant with the conduction band and expected to line up with the Fermi energy[2] only for a Si concentration above 7×10^{12} cm^{-2}. Since the Si δ-doping concentration in our sample (4×10^{12} cm^{-2}) is not high enough for the DX centers to be occupied, we can thus conclude that this effect

cannot be responsible for the PPC effect in our heterostructure.

Beall *et al.*[16] presented secondary-ion mass spectroscopy (SIMS), capacitance-voltage (CV) and local vibrational mode (LVM) measurements on δ-doped GaAs structures and found strong evidences that, at doping concentrations above 1×10^{13} cm^{-2}, only a fraction of the Si atoms was deposited on electrically active sites. The rest of the dopant precipitated as Si clusters that did not contribute to the transport properties. However, they clearly showed that for the growth temperature and Si concentration used in our sample there was no formation of such Si clusters. As a consequence, such a mechanism cannot be taken into account to explain the PPC effect observed in our sample, as already proposed by Koenraad *et al.*[3]

The presence of deep donor traps is usually invoked in order to justify any PPC in the following way: in the dark, electrons of the 2DEG are trapped in deep donor states located below the Fermi level; however, upon illumination, these electrons are transferred from the deep levels to the active region and are not efficiently recaptured by the deep states (once the light is turned off) because of the potential barriers surrounding the active region.[8,9] For the sample investigated here, a trap density of about 1×10^{16} cm^{-3} would be required, a value that is consistent with the estimated concentration of EL2 defects in MBE-grown GaAs layers.[17] This type of defect is known to have a metastable state and causes persistent sensitivity to illumination, suggesting that it might be at the origin of the PPC observed in our sample.

Whatever the specific mechanism that is at the origin of the PPC, it should also account for the changes observed in the subbands quantum mobility during the illumination process. We performed self-consistent calculations by solving the coupled Schrödinger and Poisson equations in order to simulate the electronic structure of the system in the presence of deep donor traps before exposure to any illumination ($T_{illum}=0$ s) and in the saturated stage (at $T_{illum}=1240$ s).[18] In order to simulate the dark condition at $T_{illum}=0$ s, we assumed a deep donor concentration equal to 1.0×10^{16} cm^{-3}, $N_{Si}=4.0\times10^{12}$ cm^{-2}, and $n_s=2.8\times10^{12}$ cm^{-2}. This choice was dictated by the fact that the electrons of the 2DEG are initially captured by the deep centers in the GaAs layers, outside the active region, and the δ-doped layer is strongly uncompensated ($N_{Si}\neq n_s$). The position of the Fermi level pinning at the free surface (V_S) was changed in order to obtain the best agreement between the calculated and experimentally determined subbands occupancies. Assuming that the origin of the energy scale is at the Fermi energy, the best fit of the occupancies was obtained with $V_S=250$ meV. In the saturated stage of illumination, the calculations were performed using $N_{Si}=n_s=4.0\times10^{12}$ cm^{-2} and $V_S=250$ meV. The theoretical results showed that the maximum of the electronic distribution of the $i=0$ subband, that was initially located in the InGaAs QW, moves ≈7 Å towards the δ-doped layer under strong illumination, meaning that the average distance between the carriers in the fundamental state and the ionized donors of the Si layer decreases during the illumination process, yielding a reduction of the carrier mobility in this subband. On the other hand, the influence of the illumination on the electron distribution related to the $i=1$ subband is to shift the local maximum,[19] initially located inside the δ QW, ≈11 Å away from the δ-doped layer, leading to an increase of the carrier mobility in this subband.

It is thus very clear that a systematic investigation of the transport properties of such kind of system as a function of the illumination time is important. Carrying out SdH measurements as usually, in the two extreme illumination conditions (in the dark and under continuous illumination), would certainly have led to erroneous conclusions about the number of occupied subbands and their population. Moreover, the apparent discrepancy between the data available in the literature and our experimental results about the behavior of the quantum mobility could only be solved using self-consistent calculations showing the shape and location of the electronic wave function over the δ-doped layer and the InGaAs QW. Indeed, for the very small separation adopted in our sample (20 Å), the theoretical results showed that the electron distribution is spread over both the δ and InGaAs QW's, and any slight modification of the carrier density of the subbands is enough to shift the maximum of the electronic distribution and thus modify the value of the mobility. This is no longer the case when the δ and InGaAs QW's are separated by a large distance, as already shown in the literature.

IV. CONCLUSION

Systematic Shubnikov–de Haas measurements as a function of the sample illumination time were used to determine the carrier density and quantum mobility of the occupied subbands of the two-dimensional electron gas in a silicon δ-doped InGaAs/GaAs quantum well. A persistent photoconductivity effect was detected and attributed to the presence of deep donor centers within the structure that trapped part of the conduction electrons and released them under illumination. The behavior of the quantum mobility of the different subbands was related to the band-edge modifications induced by the charge redistribution within the heterostructure. Our work clearly show that systematic illumination experiments with different exposure times can provide valuable and unambiguous information about the electronic subband structure and are very useful to elucidate transport problems in heterostructures.

The authors would like to acknowledge the financial support of FAPESP (Grant No. 2000/08794-6) and CNPq.

[1] E. F. Schubert, *Semiconductors and Semimetals*, edited by Arthur C. Gossard (Academic, New York, 1994), Vol. 40, p. 1.

[2] A. Zrenner, F. Koch, R. L. Williams, R. A. Stradling, K. Ploog, and G. Weimann, Semicond. Sci. Technol. **3**, 1203 (1988).

[3] P. M. Koenraad, F. A. P. Blom, C. J. G. M. Langerak, M. R. Leys, J. A. A. Perenboom, J. Singleton, S. J. R. M. Spermon, W. C. van der Vleuten, A. P. J. Voncken, and J. H. Wolter, Semicond. Sci. Technol. **5**, 861 (1990).

[4] G. Li and C. Jagadish, Appl. Phys. Lett. **70**, 90 (1997).
[5] Matthew Zervos, Adam Bryant, Martin Elliott, Mathias Beck, and Marc Ilegems, Appl. Phys. Lett. **72**, 2601 (1998).
[6] E. Skuras, R. Kumar, R. L. Williams, R. A. Stradling, J. E. Dmochowski, E. A. Johnson, A. Mackinnon, J. J. Harris, R. B. Beall, C. Skierbeszewski, J. Singleton, P. J. van der Wel, and P. Wisniewski, Semicond. Sci. Technol. **6**, 535 (1991).
[7] M. van der Burgt, V. C. Karavolas, F. M. Peeters, J. Singleton, R. J. Nicholas, F. Herlach, J. J. Harris, M. Van Hove, and G. Borghs, Phys. Rev. B **52**, 12 218 (1995).
[8] Ikai Lo, D. P. Wang, K. Y. Hsieh, T. F. Wang, W. C. Mitchel, M. Ahoujja, J.-P. Cheng, A. Fathimulla, and H. Hier, Phys. Rev. B **52**, 14 671 (1995).
[9] Adam Babinski, G. Li, and C. Jagadish, Appl. Phys. Lett. **71**, 1664 (1997).
[10] M. Zervos, M. Elliott, and D. I. Westwood, Appl. Phys. Lett. **74**, 2026 (1999).
[11] A. B. Henriques, Phys. Rev. B **50**, 8658 (1994).
[12] P. M. Koenraad, B. F. A. van Hest, F. A. P. Blom, R. van Dalen, M. Leys, J. A. A. J. Perenboom, and J. H. Wolter, Physica B **177**, 485 (1992).
[13] J. J. Harris, R. Murray, and C. T. Foxon, Semicond. Sci. Technol. **8**, 31 (1993).
[14] Ikai Lo, M. J. Kao, W. C. Hsu, K. K. Kuo, Y. C. Chang, H. M. Weng, J. C. Chiang, and S. F. Tsay, Phys. Rev. B **54**, 4774 (1996).
[15] For a review, see P. M. Mooney, J. Appl. Phys. **67**, R1 (1990).
[16] R. B. Beall, J. B. Clegg, J. Castagné, J. J. Harris, R. Murray, and R. C. Newman, Semicond. Sci. Technol. **4**, 1171 (1989).
[17] E. F. Schubert, *Doping in III-V Semiconductors* (Cambridge University Press, Cambridge, 1993), Chap. 11.
[18] The input of the self-consistent calculations uses parameters related to the InGaAs and GaAs materials (effective masses, dielectric constants, band gaps) and to the Si δ-doped layer (Si-doping concentration and width of the delta layer). Other parameters such as the Fermi-level pinning, background acceptor concentration, position energy of the deep donor level below the conduction band and its concentration are also needed. A detailed theoretical study about the influence of these parameters on the electronic structure of the heterostructure will be published elsewhere.
[19] The electronic carrier distribution of the second subband has two local maxima: one within the InGaAs QW and the other one located inside the δ well.